Enhancing the pharmaceutical properties of protein drugs by ancestral sequence reconstruction

Philip M. Zakas, *Emory University*
Harrison C. Brown, *Emory University*
Kristopher Knight, *Emory University*
Shannon Meeks, *Emory University*
Harold Spencer, *Emory University*
Eric A. Gaucher, *Georgia Institute of Technology*
Christopher Doering, *Emory University*

Copyright information:

Enhancing the pharmaceutical properties of protein drugs by ancestral sequence reconstruction

Philip M. Zakas[1], **Harrison C. Brown**[1], **Kristopher Knight**[2], **Shannon L. Meeks**[2], **H. Trent Spencer**[1,2], **Eric A. Gaucher**[3], and **Christopher B. Doering**[1,2]

[1]Program in Molecular and Systems Pharmacology, Laney Graduate School, Emory University, Atlanta, GA

[2]Aflac Cancer and Blood Disorders Center, Department of Pediatrics, Emory University School of Medicine, Atlanta, GA

[3]School of Biology, Institute for Bioengineering and Biosciences, Georgia Institute of Technology, Atlanta, GA

Abstract

Optimization of a protein's pharmaceutical properties is usually carried out by rational design and/or directed evolution. Here we test an alternative approach based on ancestral sequence reconstruction. Using available genomic sequence data on coagulation factor VIII and predictive models of molecular evolution, we engineer protein variants with improved activity, stability. biosynthesis potential, and reduced inhibition by clinical anti-drug antibodies. In principle, this approach can be applied to any protein drug based on a conserved gene sequence.

Many protein drugs possess suboptimal pharmacological properties yet are not amenable to standard biotechnology optimization approaches. However, the endogenous proteins these drugs are based on generally are thought to have selectively evolved over the past half-billion years to optimize functionality within the context of current or ancestral species-specific physiology. This inferred protein design landscape represents an unexplored avenue

Address correspondence to: Christopher B. Doering, PhD, 2015 Uppergate Drive, Aflac Cancer and Blood Disorders Center, Emory Children's Center, Room 450, Emory University School of Medicine, Atlanta, Georgia 30322. Telephone: 404-727-7988; Fax: 404-727-4455; cdoerin@emory.edu.

for protein drug optimization that is accessible through ancestral sequence reconstruction (ASR).

Factor VIII (FVIII) is an essential component of blood coagulation pathways, and its deficiency results in hemophilia A, the most common severe bleeding disorder. The human (h) *F8* gene was first described in 1984, and by the early 1990's several recombinant hFVIII biologics were in clinical use. FVIII infusion therapy converts this otherwise lethal disease into a clinically manageable condition, but current hFVIII biologics have several important limitations, including poor biosynthetic efficiency, short half-life, and potent immunogenicity. Despite intensive academic and commercial efforts, traditional rational design and directed evolution approaches have not yielded substantially improved FVIII biologics.

We[1–4] and others[5] have shown that extant FVIII orthologs have molecular, cellular and immune recognition properties that vary between species. This diversity may represent adaptive traits acquired throughout natural selection to promote hemostatic balance. For example, during bipedal hominid evolution, thrombosis-related mortality could have exerted selective pressure on plasma FVIII toward reduced coagulation activity. Irrespective of the validity of such evolutionary hypotheses, some ortholog-specific properties are likely to be beneficial from a pharmaceutical perspective. Previously, we exploited extant ortholog diversity to identify and engineer pharmacologically beneficial sequence determinants[6, 7]. This ortholog-scanning approach led to the creation of a highly expressed human/porcine hybrid FVIII named ET3 with 149 (11%) porcine amino acids. However, the combinatorial complexity associated with identifying the multiple, non-linear amino acid determinants blocked further humanization. The inability to sufficiently 'humanize' ortholog-hybrid molecules with xenogeneic sequences, similarly to what is done for monoclonal antibody biologics, is a major limitation of ortholog-scanning for pharmaceutical development.

ASR entails the prediction of ancient DNA and protein sequences based on information from extant sequences[8]. In contrast to ortholog scanning, it provides a higher-resolution mapping through comparisons of sequential phylogeny branches, and infers novel sequences with high potential for intended biomolecular functions as they are predicted to have once existed. This aspect of uniform functionality distinguishes ASR from all other protein drug design approaches. Advances in custom DNA synthesis now facilitate laboratory 'resurrection' and characterization of inferred ancestral proteins[9]. Recent examples of ASR applications include examination of ancestral enzyme promiscuity and functional diversification[10, 11], study of ancient receptor-ligand interactions[12], resurrection of a human pseudogene[13], and definition of an oncology drug mechanism[14]. As an approach to pharmaceutical bioengineering, ASR requires only genome information, modest computing resources, and analysis of a limited set of recombinant ancestral protein variants.

We performed FVIII ASR to infer a mammalian evolutionary tree as described previously[15] (Fig. 1a and Supplemental Fig. 1). Available extant sequence data was sufficient to accurately extend the phylogenetic tree and infer ancestral (An)-FVIII sequences beyond the class Mammalia. We synthesized inferred An-FVIII cDNAs *de novo* and expressed the An-FVIII proteins in cell lines commonly used for recombinant FVIII manufacturing.

Consistent with the hypothesis of plasma FVIII activity levels decreasing during hominid evolution, several inferred early mammalian An-FVIII (one early rodent, one early primate and one common ancestor to both) demonstrated protein expression rates ranging from 9 – 14-fold higher to those of hFVIII, and at least equivalent to the most efficiently produced recombinant FVIII molecules described previously (*i.e.* pFVIII and ET3; Fig. 1b and c). We examined An-FVIII constructs along the hominid lineage for differentials in pre-, post- and/or co-translational biosynthesis, and show that An-53, An-55 and An-56 display significantly higher FVIII production per steady-state transcript than hFVIII (Fig 1d and Supplemental Note). The mechanisms supporting increased expression of ancestral FVIII proteins are unclear, but previous reports that describe non-hFVIII residues in pFVIII and ET3 that confer increased secretion efficiency by reducing the engagement of unfolded protein response pathways offer a possible explanation[2, 6, 16]. Other processes that can improve An-FVIII biosynthesis include changes in protein synthesis or secretion efficiency, all predictably beneficial to recombinant FVIII protein production and gene therapy applications.

FVIII circulates as a pro-cofactor in a heterodimeric, A1-A2-B/ap-A3-C1-C2 domain structure. Upon proteolytic activation, the essential A2 domain quickly dissociates and FVIII becomes inactive—a natural negative feedback mechanism that prevents long-lasting hFVIII activity (Supplemental Fig. 2). Mutations that further decrease A2 stability in activated hFVIII result in reduction of coagulation potential and a mild bleeding phenotype in humans[17]. We hypothesized previously that activated hFVIII evolved to its current state of rapid A2 dissociation to reduce thrombotic risk[7]. The pharmacological correlate of this hypothesis is that stabilization of activated FVIII should result in a more potent FVIII product, an hypothesis that was supported by data from a preclinical study of murine hemophilia A[18] which showed increased cofactor activity in an in vitro thrombin generation assay and greater protection from hemostatic challenge i*n vivo* following tail transection. To assess the stability of thrombin-activated An-FVIII molecules, we monitored proteolytic activation of purified recombinant preparations for residual cofactor activity (Supplemental Fig. 3 – 4 and Table 1). Contrary to the initial hypothesis, we observed rapid decay in activated hFVIII in all primate/hominid activated An-FVIII molecules, including all ancestral proteins back to the last common mammalian ancestor. In the rodent lineage, early ancestors An-66 and -67 displayed modestly prolonged decay rates, with a $t_{1/2}$ of 3.8 and 4.4 min respectively, progressing towards the fully-extended murine activated FVIII-like with $t_{1/2}$ of 15.6 min observed for An-68 (Fig. 1e). These data suggest that the improved stability of murine activated FVIII is the result of adaptive evolutionary steps in a separate direction from the common mammalian ancestor.

In addition to production cost, the greatest obstacle to treatment of hemophilia A is the development and clinical management of anti-FVIII inhibitory antibodies. Using well-characterized anti-hFVIII murine monoclonal antibodies (MAbs) that are potent inhibitors of activated FVIII activity and display specificity for the dominant epitopes inhibited by plasma from patients with hemophilia A, we first examined An-FVIII antigenicity profiles (Fig. 2a). Despite sharing 95% identity to hFVIII, An-53 displays markedly reduced cross-reactivity to MAbs with known epitopes near or overlapping clinically-relevant epitopes in the A2 and C2 domains. All group A anti-hFVIII MAbs bind a common epitope spanning residues

484-508, and only MAbs 4A4 and G32 demonstrated a noticeable cross-reactivity to An-53[19]. Using ASR, it was possible to map and eliminate binding to MAb 4A4 by replacing a single amino acid, E434V (Fig. 2b and Supplemental Fig. 5). We then assessed the inhibition of An-53 and An-68 by hemophilia A patient plasma (which contains polyclonal anti-FVIII IgG antibodies) and observed a reduction in inhibition of >75% when compared with hFVIII. Furthermore, in 10 of 25 plasmas, the residual inhibition of the two ancestral species was either below the level of detection or within a range where therapeutic efficacy of FVIII is predicted (Fig. 2c and Supplementary Table 2). Comparison of predicted B-cell epitopes within hFVIII, ET3 and An-53 by *in silico* methods showed that ET3 stood apart from An-53 and hFVIII, whose profiles were virtually indistinguishable. These findings support the ability of ASR to guide recombinant protein bioengineering and humanization (Supplemental Fig. 6).

Based on favorable *in vitro* productivity, biochemical stability and immunogenicity data, we undertook *in vivo* pharmacology studies to assess the therapeutic potential of An-53 and An-68 as recombinant protein therapeutics or transgene components of a gene therapy product. ED_{50} estimates of 89 and 47 units/kg, were obtained for intravenously-delivered recombinant An-53 and An-68, respectively (Supplemental Table 3). A possible explanation for the apparent higher potency of An-68 is the greater stability of cofactor activity shown in Fig. 1e. The major limitation to clinical translation of gene therapy for hemophilia A is the low-level biosynthesis of hFVIII at safe vector doses as vector-directed immune responses and insertional mutagenesis represent dose-limiting toxicities for AAV and lentiviral vectors, respectively. Furthermore, current clinical gene therapy vector manufacture is inefficient compared to other biologics and the vector products costs at or near these dose limits may not be commercially feasible. Based on the enhanced *in vitro* biosynthesis data obtained for An-53, and on its higher degree of sequence similarity to hFVIII (95% identity), we compared the performance of An-53 to ET3 and hFVIII in two gene transfer settings, hydrodynamic plasmid DNA infusion and intravenous AAV vector, for delivery of liver-directed FVIII expression cassettes in hemophilia A mice. Both approaches successfully led to higher plasma FVIII activity levels with An-53 compared with ET3 or hFVIII transgenes (Fig. 2d and Supplemental Figs. 7 – 12).

In conclusion, we used ASR to identify FVIII pharmaceutical candidates with superior properties as compared with current hFVIII biologics. These properties included biosynthetic efficiency, specific activity, stability and immune reactivity. ASR is a widely accessible strategy that utilizes both known and unknown natural protein diversity to rapidly probe a protein design space that has already been refined by natural selection for beneficial properties.

ONLINE MATERIALS AND METHODS

Materials

An-FVIII cDNAs were codon optimized with human genome or liver-specific codon bias for *in vitro* and *in vivo* studies, respectively, and synthesized *de novo* by GenScript Biotech Corporation (Piscataway, NJ). SP-Sepharose, Source-Q chromatography resins, and Tricorn columns were purchased from GE Healthcare Life Sciences (Marlborough, MA).

Lipofectamine 2000, Power SYBR® PCR Master Mix, RNAlater®, reverse transcriptase and RNase inhibitor were purchased from ThermoFisher (Grand Island, NY). HEK 293T/17 cells were purchased from ATCC (Manassas, VA), BHK-M cells have been previously reported and are described further in a subsequent section [1, 2]. Serum-free AIM-V medium, Opti-mem®, and DMEM were purchased from Gibco®, ThermoFisher. Geneticin (G418) was purchased from Invitrogen, ThermoFisher. RNA and DNA isolation kits were purchased from Qiagen (Valencia, CA). Double stranded DNA fragments (gBlocks) were purchase from Integrated DNA Technologies (Coralville, IA). Polyethylenimine, Tween-80, and factor Xa chromogenic substrate were purchased from Sigma-Aldrich (St. Louis, MO). SDS-PAGE gels, protein standard, alkaline phosphatase substrate kit (AP pNPP), and Poly-Prep® columns were purchased from Bio-Rad (Hercules, CA). Pooled citrated normal plasma (FACT) and FVIII-deficient plasma were purchased from George King Biomedical (Overland Park, KS). Automated APTT reagent was purchased from Trinity Biotech (Wicklow, Ireland). Chromagenix FVIII Coatest was purchased from diaPharma (West Chester, OH). Purified factor X and human alpha-thrombin were purchased from Enzyme Research Laboratories (South Bend, IN). Factor IXa and phospholipid vesicles (PCPS) were generated and purified as previously described [7, 20, 21]. Cell culture flasks, Costar ELISA and EIA/RIA plates were purchased from Corning®, Sigma-Aldrich. Streptavidin-alkaline phosphate conjugate was purchased from Jackson Immuno Research (West Grove, PA). TransIT®-EE delivery solution was purchased from Mirus (Madison, WI). FVIII domain specific monoclonal antibodies were generated and purified as previously described [19, 22, 23]. B-domain deleted recombinant oFVIII, pFVIII, ET3 and hFVIII were generated and purified as described previously [2, 3, 6, 24]. De-identified congenital and acquired hemophilia A inhibitor patient plasma samples were provided from the Emory Inhibitor Bank. The plasmas were collected in accordance with Emory IRB protocol no. IRB00006290. AAV8-FVIII vectors were prepared by ViGene Biosciences Inc. (Rockville, MD).

Animal studies

All animal studies were performed under the guidelines set by the Emory University Institutional Animal Care and Use Committee. Exon 16-disrupted hemophilia A mice (E16) have been described previously [25]. Upon receipt of these animals from American Red Cross, the animals were backcrossed onto a C57BL/6J background. The mice are maintained as a breeding colony in the homozygous ($F8^{-/-}$) and hemizygous ($F8^{-/Y}$) state. For the hydrodynamic injection studies described, both male and female mice between 8 – 12 weeks of age were utilized without subjective bias. For the AAV gene transfer studies, only male mice were used as they are transduced more efficiently than female mice [26]. Randomization of the mice in each experiment was performed using the www.random.org "Random Sequence Generator" function. DNA and protein samples were blinded to the experimenter prior to administration to the randomized animals. Based on statistical power estimates (alpha = 0.05, power = 0.8, sigma = 0.3), and assuming expression differentials similar to those observed *in vitro* (*i.e.* 1 unit/mL) in the current study or *in vivo* in previously published studies, a minimum of 3 mice per group would be needed to determine differences. Total animal numbers (*n*) for each experiment are indicated.

Cell lines

The modified baby hamster kidney (BHK-M) cell line used in the current study has been described by our group previously. This cell line was used for the commercial development of recombinant porcine FVIII and was submitted by our colleague, Dr. Pete Lollar, to American Type Culture Collection (ATCC) and is available as catalog reference – BHK-M; hamster (PTA-4506). The human embryonic kidney 293T/17 cell line (ATCC CRL-11268) was obtained directly from ATCC.

An-FVIII sequence inference

An-FVIII sequence reconstruction was performed as described previously [15, 27]. Briefly, 47 available mammalian FVIII sequences were aligned using MUSCLE and an evolutionary tree was inferred using MrBayes (Fig. 1a) [28]. Ancestral sequences were inferred using both DNA and amino acid-based models in PAML VERSION 4.1 [29]. The multiple sequence alignment is electronically available upon request.

Biosynthetic efficiency of An-FVIII variants

HEK293T/17 and BHK-M cells were transfected with PEI or Lipofectamine 2000, respectively, in antibiotic-free media. Transiently transfected cells were washed with PBS and switched to serum-free media 48 hours after transfection and FVIII activity was measured by one-stage coagulation assay following an additional 24 h. Activity was normalized to human FVIII activity. Stable BHK-M clones were generated as previously described [1–3] and 24 – 36 clones of each FVIII construct were isolated for screening. Clones resistant to G418 but lacking detectable FVIII activity were discarded. FVIII activity was measured in serum-free media by one-stage coagulation assay and normalized to cell counts taken at the time of FVIII activity determination. RNA for subsequent steady-state transcript levels was collected following a phosphate-buffered saline (PBS) wash and storage at −80 °C in RNAlater®. Transcript levels were determined using one-step RT-PCR through interpolation to a plasmid DNA standard curve. Primers for transcript analysis are shown in Supplemental Table S4. To calculate the number of FVIII molecules generated per FVIII mRNA transcript, a generic FVIII specific activity estimate of 1 unit per 150 ng purified protein was utilized for all constructs.

Statistical analysis

All calculations were performed using SigmaPlot 13 software (Systat Software Inc., San Jose, CA). Cell-line FVIII expression comparisons made between An-FVIII constructs and hFVIII were performed using the Kruskal-Wallis one-way analysis of variance on ranks non-parametric test. Post hoc comparisons of the individual construct pairs were conducted using Dunnett's test of multiple comparisons *versus* a control group. Comparisons of FVIII concentrations following AAV8 administration were performed each week using Holm-Sidak one-way analysis of variance with all pairwise comparisons.

Purification of An-FVIII variants

The BHK-M clones displaying the greatest rate of FVIII production were expanded into triple-flasks and FVIII was collected in serum-free media and stored at −20 °C with 0.05%

sodium azide until purification. Cell debris was removed prior to storage by centrifugation at 1,000 rcf for 15 min. FVIII was purified by one- or two-stage ion exchange chromatography as previously described [2, 3]. Elution fractions were analyzed for purity via SDS-PAGE and concentration was determined by one-stage coagulation. Specific activity of homogenous FVIII samples was determined by one-stage coagulation determination compared to λ280 nm following λ320 nm and buffer corrections. Purified FVIII was aliquoted and stored at −80 °C until use for biochemical characterization.

Non-proteolytic decay via A2 domain dissociation

Activated factor VIII (FVIIIa) was measured by chromogenic assay using purified human factor IXa, human factor X, and synthetic phospholipid vesicles as described previously [2, 6, 7, 30]. Briefly, 1 nM FVIII was activated with 100 nM human thrombin for 15 s at room temperature. Desulfatohirudin (150 nM final) was added to stop the reaction and FVIII activity was measured at several time points.

Antigenicity and inhibition of An-FVIII variants

The generation and characterization of the anti-hFVIII MAbs used in the current study has been described previously [19, 22, 23, 31]. Hemophilia A inhibitor patient plasma samples were obtained from the Emory Inhibitor Bank after approval by Institutional Review Board (IRB) and written informed consent from patients, plasma samples are drawn and banked in accordance with Emory IRB protocol no. IRB00006290. Sixty-four inhibitor plasmas (52 congenital and 12 acquired) were assayed via ELISA for anti-human Ig and cross-reactivity to porcine or ancestral FVIII. Samples with an anti-human titer > 20 were included and further analyzed for inhibitor titer by modified Bethesda assay if residual volumes permitted, yielding 21 congenital and 4 acquired samples. The cross-reactivity of monoclonal anti-human FVIII antibodies (MAbs) against ancestral FVIII was measured via direct ELISA as previously described [4]. Briefly, 1.5 μg FVIII was adsorbed to an ELISA plate in 20 mM Bicine, 2 mM $CaCl_2$ pH 9.0 for 2 h and blocked with 2% BSA in 20 mM HEPES, 150 mM NaCl, 2 mM $CaCl_2$ at 4°C for at least 12 h. MAbs were selected due to A2 and C2 domain epitope recognition as well as anti-human inhibitor titers exceeding 1,000 Bethesda units (BU)/mg as previously determined [19, 23]. Biotinylated MAb at 4 μg/mL was added to the well for one h at room temperature, followed by 1:10,000 dilution of strepavidin-conjugated alkaline phosphatase in blocking buffer. Absorbance at 405 nm was measured following addition of chromogenic substrate. Mean values of triplicates were recorded and normalized to anti-hFVIII signal as percent cross-reactivity. Inhibitory titers against each FVIII construct were determined by modified Bethesda Assay as described previously [4].

Disinhibition of E434V mutant by MAb 4A4

A *de novo* synthesized DNA fragment (gBlock) containing a single point mutation E434V was inserted into An-53 by enzymes NheI and BlpI and confirmed *via* Sanger sequencing. A polyclonal population of BHK-M cells producing the E434V mutant was generated and expanded for protein collection and subsequent inhibitor testing. Inhibitor titer of Mab 4A4 was conducted using a modified Bethesda assay [32]. Briefly, E434V FVIII or purified An-53 was diluted to 0.8 – 1.2 unit/ml in conditioned serum-free supernatant from naïve BHK-M

cells and buffered with 0.1 M imidazole. FVIII and MAb 4A4 were combined and incubated at 37°C for 2 h, and residual FVIII activity was determined via one-stage coagulation assay.

In silico prediction of FVIII B-cell epitopes

B-domain deleted FVIII amino acid sequences were analyzed for potential B cell epitopes using the using the BiprePred software program [33]. Designated sensitivity and specificity thresholds were set to 0.35 and 1.3, respectively.

ED_{50} up-down efficacy determination

Hemostatic challenge was performed via tail transection as previously described [3, 34] and the ED_{50} was calculated by Dixon up-and-down method as previously described [35, 36]. Briefly, hemophilia A E16 mice were injected with saline, recombinant ancestral FVIII at varying doses, or bolus hFVIII diluted in 0.9% saline via tail vein. Mouse tails were incubated at 37 °C for 15 min prior to challenge. FVIII doses were determined *a priori* and prepared immediately preceding injection. A bleeding event was defined as blood loss (g/kg) exceeding the standard deviation of wildtype mice in an identical challenge without infused FVIII (16 mg/g body weight). Following transection, blood was collected directly in conical tubes containing pre-warmed PBS and measured by change in mass after 40 min.

In vivo FVIII gene transfer

Codon-optimized human, ET3, and An-53 FVIII were subcloned into an AAV expression cassette incorporating the liver-directed hybrid liver promoter (HLP) promoter and a synthetic polyadenylation sequence described previously [37]. Plasmid DNA was linearized outside the inverted terminal repeat (ITR) sequences and the DNA quality and quantity was assessed via gel electrophoresis prior to injection. Hydrodynamic injections were conducted as previously described [26]. Briefly, mice were weighed prior to injection and varying doses of linear plasmid was diluted into Transit-EE hydrodynamic delivery solution totaling 10% body weight. Naked DNA was delivered to hemophilia A mice age 8 – 12 weeks by tail vein injection over the course of 5–8 seconds. Blood plasma was collected at several time points following injection and FVIII activity was measured by COATEST SP assay according to the manufacturer's instructions using a standard curve generated from pooled citrated human plasma (FACT). *In vivo* specific activity of An-53 was determined by plasma activity compared to antigen levels determined by ELISA using cross-reactive anti-hFVIII murine monoclonal antibodies (MAbs) and purified recombinant An-53 as a standard. AAV8 vector was delivered intravenously *via* tail vein to 8 – 12 week old male hemophilia A mice at a dose of either 2×10^{11} or 2×10^{12} vector genomes (vg)/kg in a volume of 100 μl sterile PBS. Plasma samples were drawn weekly post AAV delivery and assayed for FVIII activity as described above.

Supplementary Material

Refer to Web version on PubMed Central for supplementary material.

Acknowledgments

References

1. Doering C, et al. Expression and characterization of recombinant murine factor VIII. Thromb Haemost. 2002; 88:450–458. [PubMed: 12353075]

2. Doering CB, Healey JF, Parker ET, Barrow RT, Lollar P. High level expression of recombinant porcine coagulation factor VIII. J Biol Chem. 2002; 277:38345–38349. [PubMed: 12138172]

3. Zakas PM, et al. Development and characterization of recombinant ovine coagulation factor VIII. PLoS One. 2012; 7:e49481. [PubMed: 23152911]

4. Zakas PM, Vanijcharoenkarn K, Markovitz RC, Meeks SL, Doering CB. Expanding the ortholog approach for hemophilia treatment complicated by factor VIII inhibitors. J Thromb Haemost. 2015; 13:72–81. [PubMed: 25315236]

5. Sabatino DE, et al. Recombinant canine B-domain-deleted FVIII exhibits high specific activity and is safe in the canine hemophilia A model. Blood. 2009; 114:4562–4565. [PubMed: 19770361]

6. Doering CB, Healey JF, Parker ET, Barrow RT, Lollar P. Identification of porcine coagulation factor VIII domains responsible for high level expression via enhanced secretion. J Biol Chem. 2004; 279:6546–6552. [PubMed: 14660593]

7. Parker ET, Doering CB, Lollar P. A1 subunit-mediated regulation of thrombin-activated factor VIII A2 subunit dissociation. J Biol Chem. 2006; 281:13922–13930. [PubMed: 16513639]

8. Zuckerkandl E, Pauling L. Molecules as documents of evolutionary history. J Theor Biol. 1965; 8:357–366. [PubMed: 5876245]

9. Merkl R, Sterner R. Ancestral protein reconstruction: techniques and applications. Biol Chem. 2016; 397:1–21. [PubMed: 26351909]

10. Risso VA, Gavira JA, Mejia-Carmona DF, Gaucher EA, Sanchez-Ruiz JM. Hyperstability and substrate promiscuity in laboratory resurrections of Precambrian beta-lactamases. J Am Chem Soc. 2013; 135:2899–2902. [PubMed: 23394108]

11. Ivarsson Y, Mackey AJ, Edalat M, Pearson WR, Mannervik B. Identification of residues in glutathione transferase capable of driving functional diversification in evolution. A novel approach to protein redesign. J Biol Chem. 2003; 278:8733–8738. [PubMed: 12486119]

12. Harms MJ, et al. Biophysical mechanisms for large-effect mutations in the evolution of steroid hormone receptors. Proc Natl Acad Sci U S A. 2013; 110:11475–11480. [PubMed: 23798447]

13. Kratzer JT, et al. Evolutionary history and metabolic insights of ancient mammalian uricases. Proc Natl Acad Sci U S A. 2014; 111:3763–3768. [PubMed: 24550457]

14. Wilson C, et al. Kinase dynamics. Using ancient protein kinases to unravel a modern cancer drug's mechanism. Science. 2015; 347:882–886. [PubMed: 25700521]

15. Gaucher EA, Govindarajan S, Ganesh OK. Palaeotemperature trend for Precambrian life inferred from resurrected proteins. Nature. 2008; 451:704–707. [PubMed: 18256669]

16. Brown HC, Gangadharan B, Doering CB. Enhanced biosynthesis of coagulation factor VIII through diminished engagement of the unfolded protein response. J Biol Chem. 2011; 286:24451–24457. [PubMed: 21606503]

17. Pipe SW, Eickhorst AN, McKinley SH, Saenko EL, Kaufman RJ. Mild hemophilia A caused by increased rate of factor VIII A2 subunit dissociation: evidence for nonproteolytic inactivation of factor VIIIa in vivo. Blood. 1999; 93:176–183. [PubMed: 9864159]

18. Leong L, et al. Noncovalent stabilization of the factor VIII A2 domain enhances efficacy in hemophilia A mouse vascular injury models. Blood. 2015; 125:392–398. [PubMed: 25331117]

19. Markovitz RC, Healey JF, Parker ET, Meeks SL, Lollar P. The diversity of the immune response to the A2 domain of human factor VIII. Blood. 2013; 121:2785–2795. [PubMed: 23349389]

20. Esmon CT, Lollar P. Involvement of thrombin anion-binding exosites 1 and 2 in the activation of factor V and factor VIII. J Biol Chem. 1996; 271:13882–13887. [PubMed: 8662922]

21. Barrow RT, Parker ET, Krishnaswamy S, Lollar P. Inhibition by heparin of the human blood coagulation intrinsic pathway factor X activator. J Biol Chem. 1994; 269:26796–26800. [PubMed: 7929416]

22. Healey JF, et al. The humoral response to human factor VIII in hemophilia A mice. J Thromb Haemost. 2007; 5:512–519. [PubMed: 17181826]

23. Meeks SL, Healey JF, Parker ET, Barrow RT, Lollar P. Antihuman factor VIII C2 domain antibodies in hemophilia A mice recognize a functionally complex continuous spectrum of epitopes dominated by inhibitors of factor VIII activation. Blood. 2007; 110:4234–4242. [PubMed: 17848617]

24. Doering CB, et al. Expression and Characterization of Recombinant Murine Factor VIII. Thromb Haemost. 2002; 88:450–458. [PubMed: 12353075]

25. Bi L, et al. Targeted disruption of the mouse factor VIII gene produces a model of haemophilia A. Nat Genet. 1995; 10:119–121. [PubMed: 7647782]

26. Brown HC, et al. Bioengineered coagulation factor VIII enables long-term correction of murine hemophilia A following liver-directed adeno-associated viral vector delivery. Mol Ther Methods Clin Dev. 2014; 1:14036. [PubMed: 26015976]

27. Gaucher EA, Thomson JM, Burgan MF, Benner SA. Inferring the palaeoenvironment of ancient bacteria on the basis of resurrected proteins. Nature. 2003; 425:285–288. [PubMed: 13679914]

28. Huelsenbeck JP, Ronquist F, Nielsen R, Bollback JP. Bayesian inference of phylogeny and its impact on evolutionary biology. Science. 2001; 294:2310–2314. [PubMed: 11743192]

29. Yang Z. PAML 4: phylogenetic analysis by maximum likelihood. Mol Biol Evol. 2007; 24:1586–1591. [PubMed: 17483113]

30. Lollar P, Parker ET, Fay PJ. Coagulant properties of hybrid human/porcine factor VIII molecules. J Biol Chem. 1992; 267:23652–23657. [PubMed: 1429706]

31. Healey JF, et al. The comparative immunogenicity of human and porcine factor VIII in haemophilia A mice. Thromb Haemost. 2009; 102:35–41. [PubMed: 19572065]

32. Barrow RT, Lollar P. Neutralization of antifactor VIII inhibitors by recombinant porcine factor VIII. J Thromb Haemost. 2006; 4:2223–2229. [PubMed: 16856973]

33. Larsen JE, Lund O, Nielsen M. Improved method for predicting linear B-cell epitopes. Immunome Res. 2006; 2:2. [PubMed: 16635264]

34. Spencer HT, et al. Lentiviral vector platform for production of bioengineered recombinant coagulation factor VIII. Mol Ther. 2011; 19:302–309. [PubMed: 21081907]

35. Parker ET, Lollar P. A quantitative measure of the efficacy of factor VIII in hemophilia A mice. Thromb Haemost. 2003; 89:480–485. [PubMed: 12624631]

36. Dixon WJ. Staircase bioassay: the up-and-down method. Neurosci Biobehav Rev. 1991; 15:47–50. [PubMed: 2052197]

37. McIntosh J, et al. Therapeutic levels of FVIII following a single peripheral vein administration of rAAV vector encoding a novel human factor VIII variant. Blood. 2013; 121:3335–3344. [PubMed: 23426947]
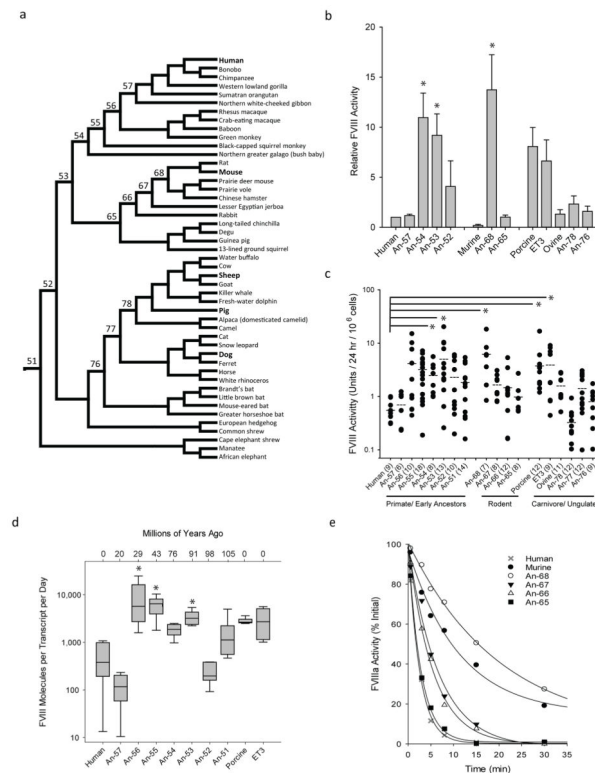
Fig. 1. An-FVIII phylogeny, recombinant productivity and cofactor stability analysis
a) A FVIII evolutionary tree and ancestral FVIII sequences were inferred from extant genomic data. The numbers shown represent the node designations for resurrected An-FVIII molecules. b) Recombinant An-FVIII production rates were determined in transient (b) and stable (c) mammalian cell expression systems. Error bars indicate sample standard deviation (s.d.), closed circles represent individual clones (with sample sizOKe in parentheses and mean as a dashed line) and asterisks highlight comparisons where *P* < 0.05. d) Biosynthetic efficiency was determined by comparison of the FVIII secretion rate to steady state mRNA transcript levels. Again, asterisks denote comparisons to hFVIII where *P* < 0.05. e) Recombinant FVIII preparations (1 nM) were activated with thrombin and residual activity was measured over time.
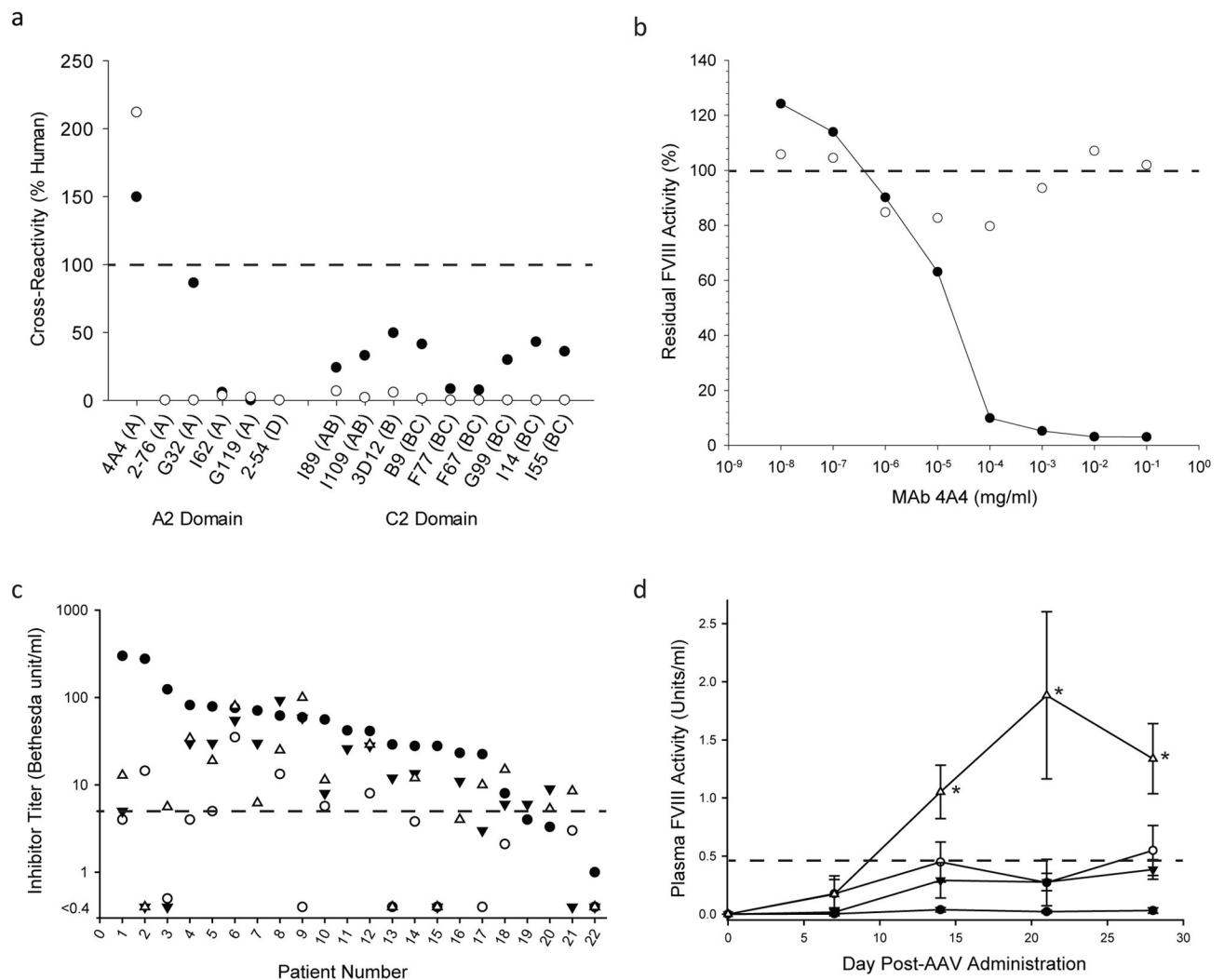
a

b

c

d

Fig. 2. An-FVIII immune safety and *in vivo* pharmacology studies
a) Cross-reactivity of inhibitory anti-hFVIII MAbs to An-53 (closed circles) and An-68
(open circles) was determined *via* direct ELISA. b) Concentration dependent inhibition of
An-53 (closed circles) and An-53 E434V (open circles) by MAb 4A4 was studied using a
modified Bethesda assay. c) Inhibition of An-53 (inverted closed triangles), An-68 (open
triangles), porcine FVIII (open circles) and hFVIII (closed circles) by hemophilia A
inhibitor patient plasma was measured using a modified Bethesda assay. The dashed line
indicates a threshold beyond which the clinical benefit of FVIII infusion therapy is
insufficient (5 BU/mL). d) Hemophilia A mice were injected with 2×10^{11} vg/kg AAV8
particles encoding hFVIII (closed circles), the bioengineered codop-hFVIII-V3 variant
(inverted closed triangles), or An-53 (open triangles) all under transcriptional control of an
identical liver-specific promoter (*n* = 4 per cohort). For comparison, a ten-fold higher dose
(2×10^{12} vg/kg) of hFVIII encoding AAV8 vector (open circles) was administered to a
separate cohort. Plasma FVIII activity measurements revealed significantly increased FVIII
levels of An-53 compared to the equivalent dose of codop-hFVIII-V3 or either dose of
hFVIII.AAV8 at weeks 2–4 (as denoted by asterisk, *P* < 0.001). The dashed line marks the

transition from hemophilia A classification to normal FVIII levels (below and above 0.45 units/ml, respectively).